UC Berkeley

UC Berkeley Previously Published Works

Title

ClURGT4 contributes to biomass accumulation in watermelon by influencing cell size and cell wall composition

Permalink

https://escholarship.org/uc/item/1114m0qr

Journal

Agriculture Communications, 4(2)

ISSN

2949-7981

Authors

Gao, Ge

Liao, Shengjin

Tian, Shouwei

et al.

Publication Date

2026-06-01

DOI

10.1016/j.agrcom.2026.100149

Copyright Information

This work is made available under the terms of a Creative Commons Attribution License, available at https://creativecommons.org/licenses/by/4.0/

Peer reviewed

eScholarship.org Powered by the California Digital Library
University of California

Agriculture Communications 4 (2026) 100149

Contents lists available at ScienceDirect

Agriculture Communications

journal homepage: www.sciencedirect.com/journal/agriculture-communications

ClURGT4 contributes to biomass accumulation in watermelon by influencing cell size and cell wall composition

Ge Gao[a,1], Shengjin Liao[a,1], Shouwei Tian[a], Xiujing Feng[a], Chen Zhang[a], Jie Zhang[a], Maoying Li[a], Shaogui Guo[a], Yongtao Yu[a], Jinfang Wang[a], Guoyi Gong[a], Haiying Zhang[a], Henrik V. Scheller[b,c,***], Yong Xu[a,**], Yi Ren[a,b,*]

[a] National Watermelon and Melon Improvement Center, National Engineering Research Center for Vegetables, Key Laboratory of Biology and Genetic Improvement of Horticultural Crops (North China), Beijing Key Laboratory of Vegetable Germplasm Improvement, State Key Laboratory of Vegetable Biobreeding, Beijing Key Laboratory of Crop Molecular Design and Intelligent Breeding, Beijing Vegetable Research Center, Beijing Academy of Agriculture and Forestry Sciences, Beijing, 100097, China
[b] Joint BioEnergy Institute and Biological Systems and Engineering Division, Lawrence Berkeley National Laboratory, Berkeley, CA, 94720, USA
[c] Department of Plant and Microbial Biology, University of California, Berkeley, CA, 94720, USA

HIGHLIGHTS

- Golgi-localized nucleotide sugar transporter ClURGT4 transports UDP-rhamnose (Rha) and UDP-galactose (Gal).
- *Clurgt4* mutants show reduced biomass, cell wall galactose (Gal), rhamnose (Rha), and galacturonic acid (GalA) in watermelon.
- Proteomic analysis revealed that ClURGT4 might control leaf and fruit size by affecting cell wall metabolism.

ARTICLE INFO

Keywords:
Fruit size
ClURGT4
Cell wall metabolism
Biomass
Watermelon

ABSTRACT

Leaf and fruit size are the crucial fitness characters for plant evolution and the agronomic traits for crop yield and quality improvement in watermelon. However, the underlying genes and molecular mechanisms for regulating fruit size and biomass remain elusive. Here, we identified a *Citrullus lanatus* UDP-rhamnose (Rha)/UDP-galactose (Gal) transporter ClURGT4, which is localized in the Golgi apparatus and has the dual functions of transporting UDP-Gal and UDP-Rha. Loss-of-function *clurgt4* mutants resulted in decreased biomass and reduced Gal, Rha, and galacturonic acid (GalA) in cell wall components. Microscopical analysis showed that ClURGT4 promoted leaf and fruit size by modulating cell expansion. Proteomic analysis revealed that several cell wall metabolism-related proteins were changed in *clurgt4* mutants. Moreover, protein glycosylation was changed in the mutants, and several of the differentially glycosylated proteins were related to cell wall metabolism. These findings elucidated that ClURGT4 might control leaf and fruit size by affecting cell wall metabolism and provided a novel case for comprehensively revealing the regulatory network of watermelon biomass.

1. Introduction

Watermelon (*Citrullus lanatus*) is an important horticultural crop that occupies an important position in fruit production and consumption in China. Leaves and fruits serve as the crucial source and sink of watermelon, and promoting the growth and development of the source and sink is of great significance for improving biomass and quality. Plant cells are enveloped by robust cell walls, which contribute to the main bulk of plant biomass [1]. Plant cell walls predominantly consist of polysaccharides, which require nucleotide sugar substrates for their biosynthesis [2]. The major nucleotide sugars in plants include UDP-glucose (Glc), UDP-rhamnose (Rha), UDP-arabinose (Ara),

* Corresponding author. Beijing Vegetable Research Center, Beijing Academy of Agriculture and Forestry Sciences, Beijing, 100097, China.
** Corresponding author.
*** Corresponding author. Joint BioEnergy Institute and Biological Systems and Engineering Division, Lawrence Berkeley National Laboratory, Berkeley, CA, 94720, USA.
E-mail addresses: hscheller@lbl.gov (H.V. Scheller), xuyong@nercv.org (Y. Xu), renyi@nercv.org (Y. Ren).
[1] Ge Gao and Shengjin Liao contributed equally to this work.

https://doi.org/10.1016/j.agrcom.2026.100149
Received 15 April 2025; Received in revised form 28 May 2025; Accepted 17 May 2026
Available online 22 May 2026
2949-7981/© 2026 The Authors. Published by Elsevier B.V. on behalf of Beijing Academy of Agriculture and Forestry Sciences. This is an open access article under the CC BY license (http://creativecommons.org/licenses/by/4.0/).

UDP-glucuronic acid (GlcA), UDP-galacturonic acid (GalA), UDP-xylose (Xyl), GDP-fucose (Fuc), and GDP-mannose (Man), all of which have a wide range of roles in plants and can function as sugar donors for (1) sucrose synthesis, (2) glycoprotein and glycolipid glycosylation reactions, (3) cell wall synthesis, and (4) secondary metabolite and hormone glycosylation [3–5]. Inhibiting the biosynthesis of nucleotide sugar substrates, such as GDP-Fuc, elicits developmental abnormalities and biochemical impairments [6]. Recent studies have also suggested that UDP-Glc may serve as a pivotal signaling molecule [7], with the genes involved in its production being upregulated in conjunction with enhanced biomass accumulation in plants [8]. Moreover, the translocation of these nucleotide sugars is a crucial step in cell wall biosynthesis, facilitated by a diverse family of nucleotide sugar transporters (NSTs) [9]. However, the molecular mechanisms by which NSTs mediate the increase in plant biomass by affecting cell wall synthesis are still not well understood, and further research is needed to fully elucidate this scientific question.

Phylogenetic analyses have revealed the presence of over 50 NSTs in *Arabidopsis thaliana*, which have been systematically classified into six distinct clades [10]. Among them, the Golgi-localized URGT1–6 in *Arabidopsis* has the dual functions of transporting UDP-Rha and UDP-galactose (Gal), and there is competition between these two substrates. The content of Gal in the leaf cell wall components of *Arabidopsis urgt1* mutants decreased, while other polysaccharide components did not change [11]. In contrast, overexpression of *AtURGT1* increased the content of Gal in the leaf cell walls. However, the decrease or increase of Gal content did not affect the plant growth and development compared with the wild type (WT). In addition, transgenic studies have conclusively demonstrated the pivotal role of *AtURGT2* in facilitating mucilage formation during seed development. Furthermore, the UDP-xylose transporter (UXT) family, comprised of three UXT proteins, has been recognized for its capability to transport UDP-Xyl and a minor fraction of UDP-arabinopyranose. Cell wall compositional analyses have revealed that *uxt* loss-of-function mutants exhibit a marked decrease in the content of xylose-associated polysaccharides, including xylan and glucuronoxylan, accompanied by an elevation in proteoglycan levels, as compared with wild-type plants [12]. In the context of the rice blast fungus *Magnaporthe oryzae*, two NSTs (NST1 and NST2) have been thoroughly investigated. NST1 was found to be instrumental in the transport of both Man and Glc, whereas NST2 specifically mediated the transport of Man [13]. The deletion of these NSTs resulted in a decline in the corresponding soluble sugar levels. Additionally, the NST mutants displayed reduced levels of external glycoproteins, leading to the exposure of underlying chitin and the subsequent activation of the host defense mechanisms [13]. Currently, research on NSTs has mainly focused on model plants, and the molecular mechanisms of NSTs have not been reported yet. Therefore, a comprehensive and systematic study is required to reveal the function of NST and its regulatory network in fruit crops. This knowledge is important for developing high-yielding and superior watermelon cultivars and accelerating breeding efficiency.

In our study, we reported the identification and characterization of a NST ClURGT4 in watermelon. We found that ClURGT4 transported both UDP-Gal and UDP-Rha. Mutation of ClURGT4 resulted in smaller leaf and fruit size, along with reduced biomass, and correlated with changes in Golgi proteins and glycosylated proteins involved in cell wall metabolism. Our findings provide new insights into the regulatory pathway of fruit size and biomass in watermelon mediated by cell wall metabolism.

2. Materials and methods

2.1. Plant materials and growth conditions

The watermelon (*Citrullus lanatus*) inbred variety “zhongzijingmu” (cultivar), the transgenic plants in this background, and the wild species PI296341 were grown in a plastic greenhouse under a temperature range of 25–35 °C in Beijing, China. The female flowers were pollinated manually on the opening day and labeled upon the arrival of bloom. Whole plant and watermelon fruit were harvested at 20 days after pollination (DAP), and 26 DAP was used for biomass, fruit size, cell wall monosaccharide, and proteome analysis. Specifically, three independent plants or fruits and three biological replicates were used to evaluate the above content.

Nicotiana benthamiana (Domin) plants were cultivated in pots within a growth chamber, where environmental conditions were stringently controlled to ensure optimal growth and development (25 °C, 16 h light, 8 h dark).

2.2. Clustered regularly interspaced short palindromic repeats (CRISPR)/Cas9 vector construction and plant transformation

To construct the CRISPR/Cas9 vector, the designed sgRNA from the first exon of the *ClURGT4* gene was ligated into the pBSE406-GFP vector. The *Agrobacterium tumefaciens* strain EHA105, harboring the designated DNA construct, was employed for the transformation process as outlined in a previous study [14]. This involved an initial step of cultivating surface-sterilized watermelon seeds in the dark for four days. Subsequently, the regenerated adventitious buds were carefully excised and transferred onto a specialized, selective elongation medium containing 0.1 mg/L 6-benzyladenine, 0.01 mg/L α-naphthalene acetic acid, and 2 mg/L Basta (glufosinate ammonium) (Coolaber, Beijing, China). To identify CRISPR/Cas9-mediated indel mutations, a genotyping analysis was conducted using a pair of primers specifically designed to flank the sgRNA target site, with the forward primer positioned 5’ upstream and the reverse primer located 3’ downstream (Supplementary Table 1). From this selection, Cas9-free T_2 progeny and homozygous *clurgt4* mutants were isolated and harvested for subsequent phenotypic characterization. As a negative control, transgenic plants displaying no Basta resistance and lacking any editing events within the same segregating population were included in the study.

2.3. RNA extraction, cDNA synthesis, and gene expression analysis

The total RNA was extracted and purified from different watermelon tissues and fruits of wild-type and *clurgt4* mutants utilizing the RNA isolation kit (Cat#CW0581, CWbio. Co. Ltd., Beijing, China) according to the manufacturer’s protocol. Subsequently, 1000 ng of the total RNA was utilized to synthesize first-strand cDNA, employing the PrimeScript™ RT Master Mix (Takara, Dalian, China). We conducted RT-qPCR analyses using SuperReal PreMix Plus (SYBR Green) (Takara, Dalian, China), following the manufacturer’s protocol. The relative expression levels of the target genes were calculated using the $2^{-\Delta\Delta Ct}$ method, with three biological and technical replicates for accuracy. As internal control genes, we employed the actin gene (ID: *Cla97C02G026960*) from watermelon [15]. The RT-qPCR primers used in this study are listed in Supplementary Table 2.

2.4. Measurements of soluble solids

The soluble solid content (SSC) was measured using a portable ATC-1E refractometer (model PAL-1; ATAGO Co., Ltd., Tokyo, Japan) by extracting juice from the core of each watermelon flesh, ensuring a representative and accurate assessment of the sample.

2.5. Phylogenetic analysis

Phylogenetic trees were constructed utilizing the neighbor-joining method implemented within the Clustal X 2.1 software, with a bootstrap value rigorously set to 100 replicates to ensure the robust evaluation of the reliability and statistical significance of the various phylogenetic groupings. Subsequently, the resulting tree files were

visually rendered and refined for clarity and precision using MEGA X software.

2.6. Transmembrane structural domain analysis

Transmembrane domain analysis of ClURGT4 was done using Protter (https://wlab.ethz.ch/protter) [16].

2.7. Heterologous expression, reconstitution, and in vitro assay of transport activities

The uracil-auxotrophic yeast strain INVScI was transformed following the guidelines provided by the manufacturer (Life Technologies, Carlsbad, California, USA). Subsequently, microsomal membranes were isolated from a 500 mL culture medium. The yeast microsomal proteins were integrated into liposomes through detergent solubilization and rapid detergent removal. This procedure utilized acetone-purified soybean L-α-phosphatidylcholine (Avanti Polar Lipids, Alabaster, USA), maintaining a precise lipid/protein ratio of 13:1, and utilized octyl-β-glucoside as the detergent. The resultant liposomes were then carefully diluted in a reconstitution buffer and utilized for the quantitative assessment of transporter activity at a controlled temperature of 25 °C, with specific time intervals and utilizing appropriate nucleotide sugar substrates. The reactions were terminated through gel filtration on Sephadex G50 (GE Healthcare, Chicago, USA) columns. The captured nucleotide sugars were extracted following the well-established protocol [17]. The freeze-dried extracts were subsequently dissolved in 1 mL of 10 mM ammonium bicarbonate and further purified according to the carbon column purification method [18]. The purified extracts were lyophilized once more and then resuspended in 200 μL of liquid chromatography-mass spectrometry (LC-MS) grade water, ensuring the highest degree of purity and suitability for analysis. Kinetic parameters were calculated using the Prism 6 (GraphPad), providing a comprehensive understanding of functional characteristics and activities of the transporter.

2.8. Microscopy

The microscopic architecture of the leaf and fruit cells was evaluated, adhering to the established protocol [19]. Briefly, a 1 mm^3 section of flesh tissue centered around the equatorial region of the fruit was immersed in FAA solution (a mixture comprising 40 % formaldehyde, 70 % ethanol, and glacial acetic acid) for 48 h. The flesh tissues were then dehydrated through an ethanol gradient. Next, the samples were sequentially immersed in 50 % (tert-butanol: paraffin = 1:1, v/v), 75 % (tert-butanol: paraffin = 1:3, v/v), and 100 % paraffin for 6 h, and the processed samples were embedded in melted paraffin. The paraffin blocks were sectioned with a thickness of 7–10 μm using a microtome (Leica RM2245, Leica Biosystems, Nussloch, Germany). The sections were stained with 0.5 % (w/v) toluidine blue O for 2 min, washed twice with distilled water, and treated with 0.5 % (v/v) acetic acid solution for 1 min. Finally, the stained sections were dehydrated by an ethanol gradient. Once thoroughly dried, the samples were captured under the microscope using a U-TV 0.63XC imaging system (Olympus, Tokyo, Japan), affording the clear and detailed visualization of the intricate microstructure of the fruit cells.

2.9. Cell wall monosaccharide analysis

Cell wall polysaccharides were prepared as alcohol insoluble residues (AIR) and lyophilized. After polysaccharide hydrolysis in 2 M trifluoroacetic acid (TFA) at 120 °C, monosaccharide determination was performed using high-performance anion exchange chromatography with pulsed amperometric detection as previously described [11].

2.10. Golgi apparatus proteome and glycosylated proteome analysis

Golgi vesicles from watermelon fruit were isolated using the Invent Golgi Apparatus Extraction Kit (Invent Biotechnologies, catalog number PG-049, Plymouth, USA), and Golgi proteins were extracted for Golgi proteomic analysis. Total proteins from watermelon fruits were extracted following the method of Yang et al. [20] with three biological replicates for glycosylated proteomic analysis. This process used the label-free method [21] for protein extraction and quantification. Protein concentration was determined using the Bradford method [22], and the quality of protein extracts was checked by SDS-PAGE. Next, 100 μg of extracted protein was digested with trypsin and desalted. For glycosylated peptide enrichment, 0.5 % TFA aqueous solution was used to activate the hydrophilic interaction liquid chromatography (HILIC) enrichment column, followed by equilibration in binding buffer (80 % acetonitrile, 5 % formic acid (FA)). The binding buffer was added to the peptide sample, mixed by pipetting, and incubated for 2 h. After passing the sample through the column, the column was washed three times with the binding buffer. The glycopeptides were eluted with 0.5 % FA into a new 1.5 mL tube, and the column was eluted again with 5 % acetonitrile and 0.5 % FA; the combined eluate was lyophilized. Tryptic peptides were analyzed by Nanoflow LC-MS/MS on a quadrupole Orbitrap mass spectrometer (Q Exactive HF-X, Thermo Fisher Scientific, Bremen, Germany) coupled to an EASY nLC 1200 ultra-high-pressure system (Thermo Fisher Scientific) via a nano-electrospray ion source. All RAW files were analyzed using the Proteome Discoverer suite (version 2.4, Thermo Fisher Scientific). The spectra derived from each individual fraction underwent separate searches against the watermelon-specific database. To ensure high accuracy, a percolator was employed to filter peptide spectral matches and peptides, achieving a stringent false discovery rate (FDR) threshold of less than 1 %. Following spectral assignment, the identified peptides were assembled into proteins, which were then subjected to an additional layer of filtering based on the cumulative probabilities of their constituent peptides, ultimately achieving an overall FDR of 1 %. For functional annotation, Gene Ontology (GO) and InterPro (IPR) analyses were performed using the InterProScan-5.0 program, querying against a comprehensive non-redundant protein database. Furthermore, to gain insights into protein families and metabolic pathways, the databases COG (Clusters of Orthologous Groups) and KEGG (Kyoto Encyclopedia of Genes and Genomes) were utilized, providing a deeper understanding of the biological context and functional roles of the identified proteins.

2.11. Statistical analysis

The data were analyzed using the advanced statistical capabilities of SPSS version 22.0. This comprehensive analysis encompassed the calculation of average values, standard deviations, and the identification of statistically significant differences among the various samples. The data were presented as mean ± standard deviation, and significant differences were determined using independent *t*-tests and noted with asterisks ($^*P < 0.05$, $^{**}P < 0.01$).

3. Results

3.1. ClURGT4 was widely expressed and located in the Golgi apparatus

Arabidopsis encodes six proteins in the family of URGT, forming two distinct clades: subclade A (AtURGT1 to AtURGT3) and subclade B (AtURGT4 to AtURGT6). Subclade A shares only 46 %–48 % identity in amino acid sequences with subclade B in *Arabidopsis* [11], and these differences indicate that the two distinct subclades may have different functions. AtURGT1 and AtURGT2 in subclade A are involved in pectic galactan synthesis and seed mucilage formation, respectively [11]. In addition, recent research has associated AtURGT4 and AtURGT6 with rhamnogalacturonan I (RG-I) biosynthesis in *Arabidopsis* [23]. Herein,

four *ClURGT* genes were identified in the watermelon genome. Among them, ClURGT4 shared about 79 % amino acid identity and 71 % coding sequence similarity with the *Arabidopsis* AtURGT4 in subclade B (Fig. 1a). ClURGT4 had 10 predicted transmembrane domains (Fig. 1b). Moreover, we examined the tissue-specific expression pattern of *ClURGT4* through transcriptome data (http://cucurbitgenomics.org/organism/21), and found that it was widely expressed in various reproductive and vegetative organs, including seed, floral bud, flower, root, leaf and fruit, and was expressed notably at a relatively higher level in 25-DAP seed and 26-DAP cultivated fruit (Fig. 1c). Moreover, we also validated the reliability of transcriptome data through RT-qPCR (Supplementary Fig. 1).

To corroborate the subcellular localization of ClURGT4, we fused the *ClURGT4* sequence with the green fluorescent protein (GFP) gene and expressed the corresponding fusion protein transiently in tobacco leaves. The green fluorescence was well resolved in the Golgi apparatus (Fig. 1d), and colocalized with the known *cis*-Golgi marker α-mannosidase. These results demonstrate that ClURGT4 is a Golgi-located NST and widely expressed in different tissues.

3.2. *ClURGT4 was a UDP-Gal and UDP-Rha transporter*

We heterologously expressed ClURGT4 in yeast to identify the substrate transported by ClURGT4, and vesicles were extracted and reconstituted to preload uridine 5'-phosphate (UMP), a required exchange substrate with nucleotide sugars for most NSTs. The results of kinetic parameters showed a *Km* of 57.6 μM and a V_{max} of 3.2 nmol/s/mg protein for transporting UDP-Gal and a *Km* of 67.1 μM and a V_{max} of 3.9 nmol/s/mg protein for transporting UDP-Rha (Fig. 2a and b). The levels of UDP-sugars are in the micromolar range in plant cells [24]. Therefore, the estimated *Km* values of UDP-Gal and UDP-Rha for ClURGT4 are within the physiological range in plant tissues. In summary, the ClURGT4 protein showed UDP-Gal and UDP-Rha transport activities as measured by time-dependent uptake of UDP-Gal/UDP-Rha, while no activity was detected when the empty vector control was expressed (Fig. 2c and d).

3.3. *ClURGT4 contributed to biomass accumulation in watermelon*

The functions of ClURGT4 in vivo were illustrated using CRISPR/Cas9 gene editing technology, and *clurgt4* mutants from cultivar 'zhongzijingmu' were generated. Two T_2 mutant lines, *urgt4-1* and *urgt4-2*, harboring a 26-nt and a 2-nt deletion, respectively, in the second exon of the coding region near the protospacer-adjacent motif (PAM) site were analyzed (Fig. 3a). And RT-qPCR results showed that the transcription level of *ClURGT4* was significantly downregulated in *clurgt4* mutants compared with WT (Fig. 3c). Shorter main branches and poor growth vigor were observed in the T_2 populations with *clurgt4* homozygous alleles, compared with WT. Smaller fruit size was observed in *clurgt4* mutants at 20 DAP and 26 DAP (Fig. 3b). Compared with WT, the fresh weight (FW) and dry weight (DW) of the fruit at 26 DAP in the two lines of *clurgt4* mutants decreased by approximately 30 % and 35 %, respectively, along with a 25 % reduction in fruit water content (Fig. 3d and e, and Supplementary Fig. 2). About 10 % decrease in SSC was observed in *clurgt4* mutants (Fig. 3f). Altogether, our results demonstrate that ClURGT4 is essential for normal development of watermelon fruit.

Compared with WT, *clurgt4* mutants had smaller leaf and fruit sizes (Fig. 4a and b). Paraffin sections revealed the cell diameters and morphology of leaf and fruit. As shown in Fig. 4c–h, compared with WT, mutation of the *ClURGT4* gene resulted in restricted cell wall expansion, leading to approximately 23 % and 30 % decrease in cell diameters of leaf and fruit (Fig. 4i and j). Consistently, the transverse and longitudinal diameters of the *clurgt4* mutant fruits at 20 DAP and 26 DAP also decreased by about 30 % compared with the wild-type fruit (Supplementary Fig. 3), indicating that the reduction in leaf and fruit size in *clurgt4* mutant was caused by a defect in cell expansion rather than in cell proliferation.

3.4. *Cell wall Gal, Rha, and GalA contents were reduced in clurgt4 mutants*

URGTs are mainly responsible for transporting nucleotide sugars from the cytosol into the Golgi lumen, which is a key process in cell wall biosynthesis. The cell wall is a complex and diverse structure that is

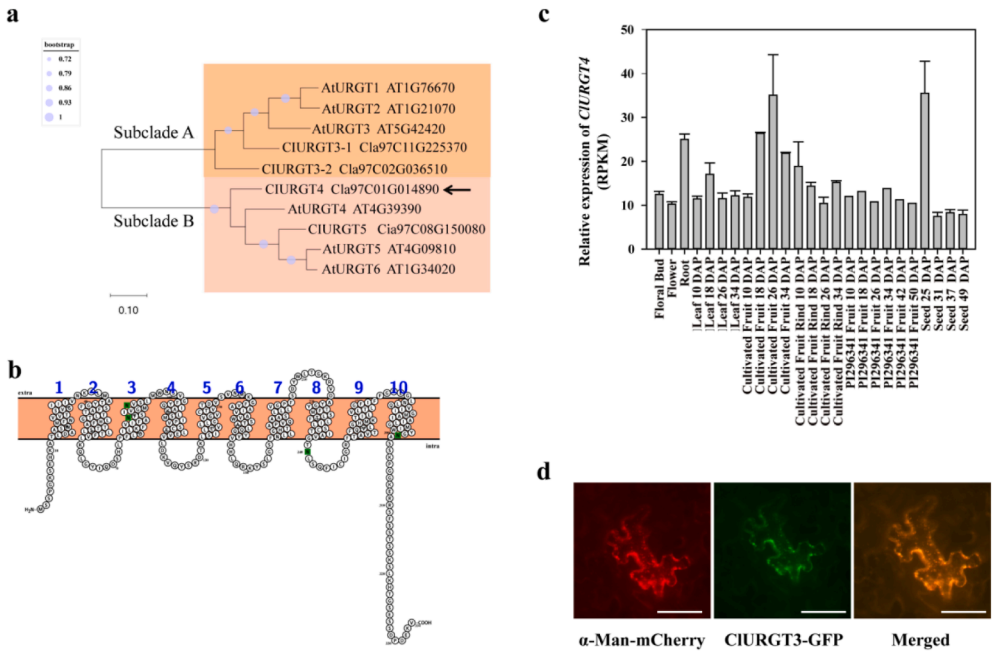


Fig. 1. Identification and analysis of ClURGTs in watermelon. (**a**) A neighbor-joining phylogenetic tree of *Arabidopsis* (At) and watermelon (Cl, *C. lanatus*) URGTs. ClURGT4 is marked by a black arrow in subclade B. (**b**) Analysis of ClURGT4 transmembrane domains. (**c**) Expression pattern of *ClURGT4* in different tissues of watermelon according to transcriptome data. (**d**) Subcellular localization of the ClURGT4 protein. Scale bars: 50 μm.

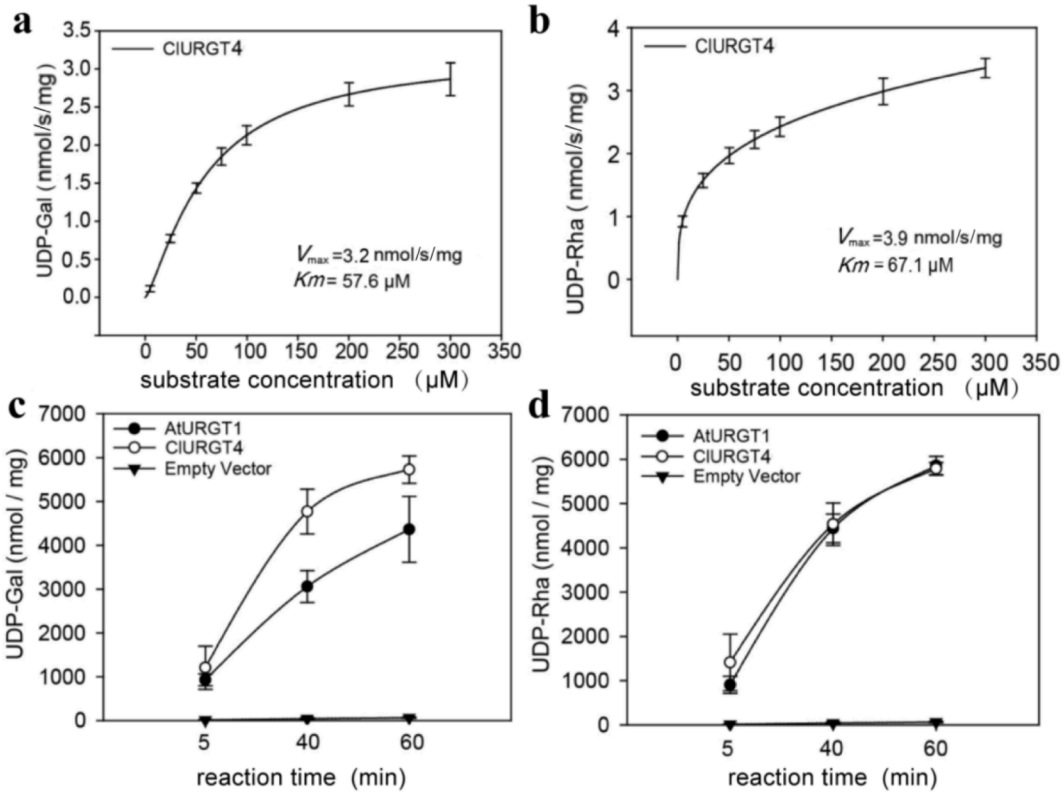


Fig. 2. Time- and concentration-dependent nucleotide sugar uptake into proteoliposomes. Kinetics of (**a**) UDP-Gal and (**b**) UDP-Rha transport. Proteoliposomes, preloaded with UMP, were incubated with their respective nucleotide sugar at different concentrations (0–300 μM) for 3 min at 25 °C. Time courses of (**c**) UDP-Gal and (**d**) UDP-Rha uptake. Proteoliposomes, preloaded with UMP, were incubated with the respective nucleotide sugar at a concentration of 100 μM for the indicated time points at 25 °C. Values were normalized to the ClURGT4 protein content present in the proteoliposome preparations and were represented as mean ± SD of three independent experiments. Yeast transformed with the empty pYES-DEST52 vector was used as a control.

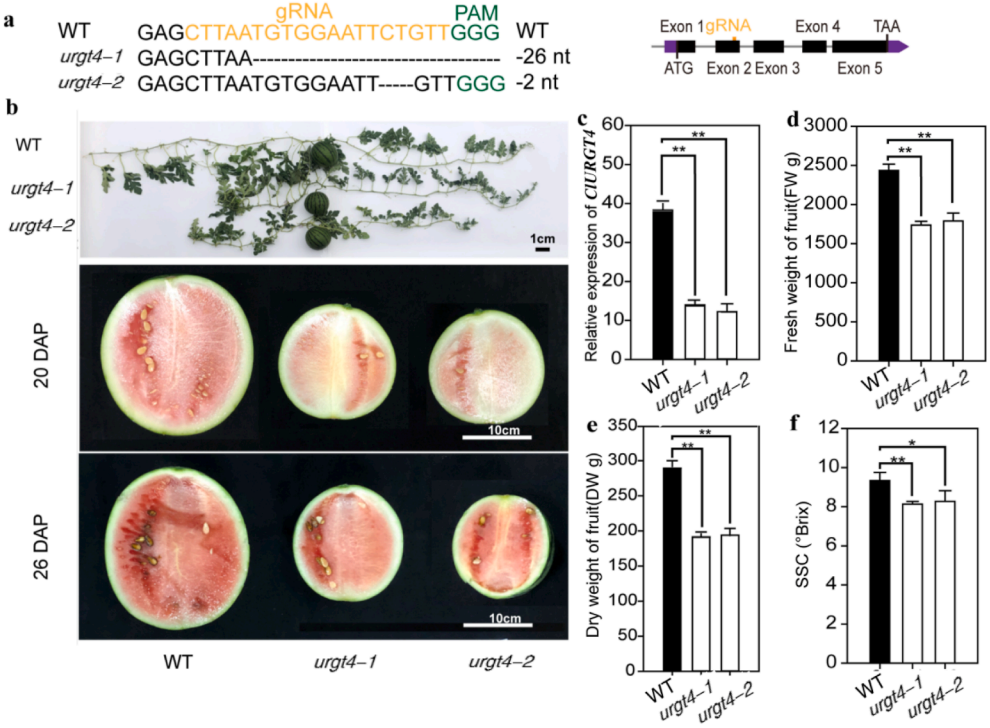


Fig. 3. Phenotypic observation of *clurgt4* plants and fruits, as well as determination of biomass and sugar content. (**a**) CRISPR/Cas9-generated *clurgt4* alleles. The schematic diagram illustrates sgRNA targeting the second exon of ClURGT4, which results in a null mutation of ClURGT4. (**b**) Phenotype of plant and fruit development of *clurgt4* mutation lines and WT at 20 DAP and 26 DAP. (**c**) The expression level of *ClURGT4* in WT and *clurgt4* mutants. (**d**) The FW of the fruit in the two lines of *clurgt4* mutants and WT. (**e**) The DW of the fruit in the two lines of *clurgt4* mutants and WT. (**f**) Analysis of SSC (°Brix) in *clurgt4* mutants and WT at 26 DAP. Average values ± SD for n = 3 independent biological replicates are shown. **t*-test significant at $P < 0.05$, ***t*-test significant at $P < 0.01$.

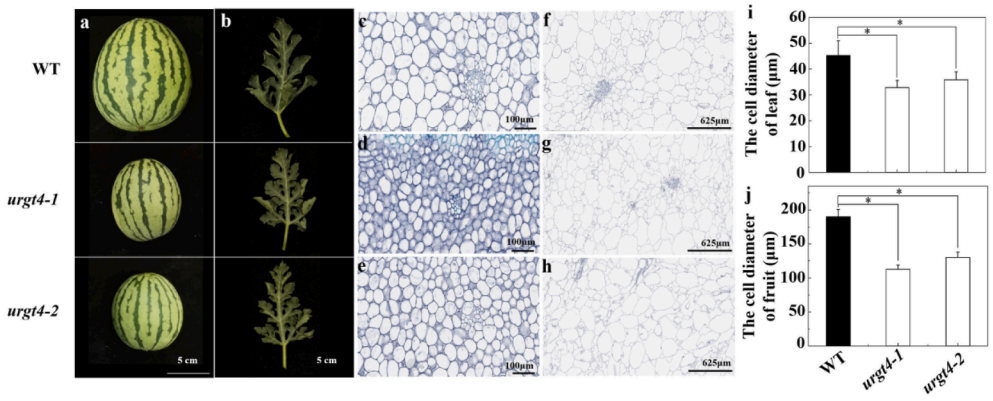


Fig. 4. Number and size of leaf and fruit cells in WT and *clurgt4* mutants. (**a**) Phenotype of WT and *clurgt4* fruits. (**b**) Phenotype of WT and *clurgt4* leaves. (**c**–**e**) Observation of changes in the number and size of leaf cells in (**c**) WT, (**d**) *clurgt4-1*, and (**e**) *clurgt4-2* using paraffin sections. (**f**–**h**) Observation of changes in the number and size of fruit cells in (**f**) WT, (**g**) *clurgt4-1*, and (**h**) *clurgt4-2* using paraffin sections. (**i**) The average diameters of WT and *clurgt4* mutant leaf cells in the same field of view were calculated based on paraffin sections using ImageJ 1.x software. (**j**) The average diameters of WT and *clurgt4* mutant fruit cells in the same field of view. Average values ± SD for n = 3 independent biological replicates are shown. **t*-test significant at $P < 0.05$.

mainly composed of polysaccharides [11]. Based on this, we conducted a monosaccharide composition analysis of cell wall residues between *clurgt4* and WT fruits. The result of the monosaccharide composition analysis of cell wall residues showed that Gal, Rha, and GalA contents were significantly decreased in *clurgt4* fruit (Table 1), indicating that ClURGT4 plays an important role in regulating the polysaccharide components of the cell wall.

3.5. Golgi apparatus proteome and glycosylated proteome were explored to identify the proteins altered in clurgt4 mutants

Most non-cellulosic cell wall polysaccharides are synthesized in the Golgi apparatus using nucleotide sugars predominantly produced in the cytosol. Our findings showed that ClURGT4 was located in the Golgi apparatus and it was identified as a UDP-Gal and UDP-Rha transporter. To explore the molecular mechanisms of reduced biomass and smaller fruit size in *clurgt4* mutants, we performed Golgi proteome analysis to investigate whether ClURGT4 knockout affected cell wall metabolism-related proteins at the proteomic level (**Supplementary Data Set 1**). Based on the previous study, the degradation and relaxation of cell walls were positively correlated with cell enlargement, and downregulation of proteins such as expansin, beta-D-glucosidase, and pectin lyase repressed cell wall degradation [25]. Receptor kinases have also been reported to be involved in regulating cell size [26,27]. Some proteins were significantly enriched in the pathways of cell wall degradation and expansion, as well as receptor kinases (Fig. 5a).

The Golgi proteomics results suggested that the loss-of-function of ClURGT4 impacted cell wall remodeling by downregulating proteins essential for cell expansion. Differentially expressed proteins were enriched in proteins involved in posttranslational modification and protein turnover (Supplementary Fig. 4). In view of that, we further conducted glycoproteomics to investigate whether the mutated ClURGT4 affected the abundance and N-glycosylation of cell wall metabolism-related glycoproteins. The results revealed that a large number of differentially abundant proteins were enriched in carbohydrate transport and metabolism, and cell wall modification (Supplementary Fig. 5, **6**). Among them, two peroxidases (Cla97C10G197400 and Cla97C02G049870) were upregulated, while a pectin lyase protein (Cla97C05G107600) was downregulated in *clurgt4* mutants (Fig. 5b). The two peroxidase proteins were glycosylated at amino acid positions 209 and 140, respectively, and the pectin lyase protein was glycosylated at amino acid positions 332, and their sugar chains contained different amounts of HexNAc, hexose, Fuc, and Xyl (**Supplementary Data Set 2**). During the intricate process of lignification, monolignols are intricately orchestrated to be secreted into the cell wall, where they subsequently undergo polymerization through a series of oxidative reactions, as demonstrated by Vanholme et al. [28]. Enzymes such as laccases and cell wall peroxidases generate reactive oxygen species (ROS), which play a crucial role in this process. These ROS not only facilitate the crosslinking of monolignols into the complex lignin polymer, but also contribute significantly to reinforcing the structural integrity of the cell wall, thereby enhancing its strength and simultaneously restricting further cell extension [25]. Above all, ClURGT4 mutation resulted in upregulation of peroxidases and downregulation of pectin lyase, and changed their glycosylation pattern. This may have contributed to decreasing cell wall degradation and increasing lignification, ultimately leading to smaller leaves and fruits, reducing watermelon biomass in *clurgt4* mutants.

4. Discussion

In this study, NST URGTs were identified in watermelon. Among them, ClURGT4 is widely expressed in different tissues of watermelon, with 10 transmembrane domains and localized in the Golgi apparatus (Fig. 1). These characteristics are consistent with previously reported NSTs [11]. The Golgi apparatus is the main site for the synthesis of cell wall polysaccharides. In plant cells, the Golgi apparatus can synthesize and secrete various polysaccharides, which are important components of the cell wall. Moreover, the Golgi apparatus not only synthesizes polysaccharide components of the cell wall, but also processes and modifies these components [29]. For example, the Golgi apparatus binds proteins with polysaccharides to form glycoproteins, which are

Table 1
Monosaccharide contents of cell wall residues from the fruits of WT and *clurgt4* plants (μg/mg).

	Rhamnose	Fucose	Arabinose	Xylose	Mannose	Galactose	Glucose	GalA	GlcA
WT	8.2 ± 0.3	6.0 ± 0.6	11.0 ± 1.4	43.9 ± 4.7	10.6 ± 2.3	130.4 ± 5.0	24.6 ± 2.6	21.2 ± 3.5	0.9 ± 0.1
urgt4-1	6.2 ± 0.2*	5.4 ± 0.6	9.6 ± 0.5	39 ± 4.9	11.4 ± 0.8	99.2 ± 12.8*	28.2 ± 3.1	15.8 ± 3.1*	1.0 ± 0.1
urgt4-2	5.0 ± 1.0*	5.5 ± 1.6	9.1 ± 1.6	40.5 ± 11.4	10.8 ± 2.5	86.2 ± 18.2*	22.6 ± 5.6	13.1 ± 3.1*	0.8 ± 0.2

Note: The amounts of non-cellulosic monosaccharides were determined by high-performance anion exchange after TFA hydrolysis. * Significantly decreased (*t*-test at $P < 0.05$) compared with WT (n = 3) ± SD.

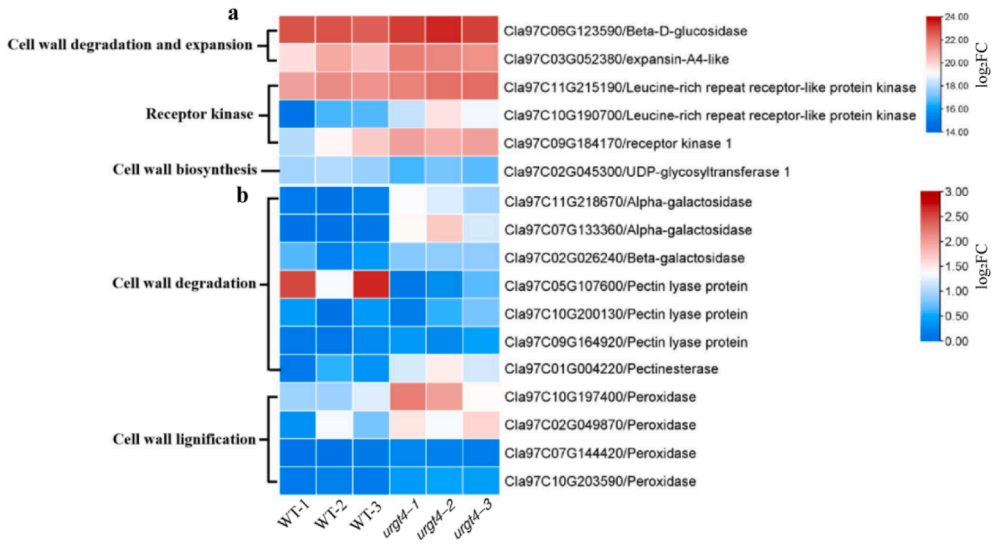


Fig. 5. Heat maps showing the differential proteins involved in cell wall metabolism in the fruits of WT and *clurgt4* mutants. (**a**) Differential proteins from the Golgi apparatus proteome. (**b**) Differential proteins from the glycosylated proteome. The color of the heat map represents the level of protein accumulation, red represents higher protein accumulation, blue represents lower protein accumulation, and white represents moderate protein accumulation.

important components of the cell wall and can enhance the strength and toughness of the cell wall [30]. In summary, ClURGT4, localized in the Golgi apparatus, as the main site for the synthesis and modification of cell wall polysaccharides, may play a role in the formation and maintenance of the cell wall, thereby regulating the structure and function of the cell wall. However, although NSTs are essential for the synthesis of cell wall polysaccharides in the Golgi apparatus, research on their functions is relatively scarce [3,5,31]. In this study, we found that ClURGT4 had the dual functions of transporting UDP-Gal and UDP-Rha (Fig. 2). This result is consistent with the reported function of AtURGT1–6 to transport UDP-Gal and UDP-Rha in *Arabidopsis* [11]. In addition, several NSTs for transporting various nucleotide sugars (e.g., UDP-Xyl, UDP-arabinofuranose, UDP-uronic acids, GDP-Fuc, GDP-L-Gal, UDP-N-acetylglucosamine) have already been characterized [12,32]. In the future, further research on the biological function of NSTs in the growth and development of horticultural crops is necessary.

To comprehensively understand the function of ClURGT4 in watermelon, we generated loss-of-function mutants. The *clurgt4* mutants showed a reduction in cell wall Gal, Rha, and GalA contents (Table 1). Study has shown that overexpression of a cytosol-localized UDP-Rha synthase (RHM1) can increase the content of Rha in leaf cell wall of *Arabidopsis* [33], indicating that UDP-Rha synthesis, rather than UDP-Rha transport affects cell wall Rha amount. It was observed in *Arabidopsis* that AtURGT1 provides Gal for pectin side chain biosynthesis, but not for xyloglucan galactosylation, whereas AtURGT2 appears to provide Rha for RG-I backbone biosynthesis, even though the two proteins have very similar dual activities in vitro [11]. It is possible that different URGT isoforms preferentially provide UDP-Gal or UDP-Rha to different acceptors, possibly through metabolism formation and protein-protein interactions. In this study, ClURGT4 could transport both UDP-Gal and UDP-Rha, and there were significant changes in Gal, Rha, and GalA contents in the cell wall polysaccharides of *clurgt4* knockout lines. ClURGT4 belongs to URGT clade B, whereas AtURGT1 and AtURGT2 belong to clade A. ClURGT4 is more similar to *Arabidopsis* AtURGT4, AtURGT5, and AtURGT6, and AtURGT4 and AtURGT6 have been proven to be involved in RG-I synthesis in seed mucilage by reducing Rha and GalA content [15]. This indicates that the URGTs of clade B family, especially URGT4, participate in controlling various growth and development processes of different plants by affecting the content of Rha and GalA. In vitro and in vivo experiments have also demonstrated functional similarities and differences of URGT4 among different species. Previous study has shown that the RG-I backbone is mainly composed of GalA-Rha repeats, and there is a significant amount of RG-I in *Arabidopsis* seed mucilage [34]. This indicates that the lower GalA and Rha contents in the *clurgt4* mutants may lead to obstruction of RG-I synthesis. In addition to the decrease of polysaccharide contents in cell wall, the leaf and fruit size of *clurgt4* mutants were smaller than those of WT (Figs. 3 and 4). We think this is unlikely to be a direct result of the change in cell wall Gal, Rha and GalA, since *Arabidopsis* mutants with more substantial changes in cell wall Gal show no obvious growth changes [35–37]. Consistently, pectin is composed of three major polysaccharides, including homogalacturonan (HG), RG-I, and RG-II [38]. Among them, Rha and GalA are important components of the RG-II side chain, and RG-II plays an important role in controlling normal plant growth and development [39]. Therefore, we speculate that the decrease in GalA and Rha contents in the *clurgt4* mutant may inhibit RG-II synthesis to decrease watermelon plant biomass and fruit size. In the *clurgt4* mutants, both fruit size and cell diameter decreased by approximately 30 %, with the reduction magnitudes being largely consistent. This indirectly suggests that defective cell expansion, rather than altered cell proliferation, is the primary cause of the reduced fruit size. However, direct cell counting or genome DNA content analysis is still required to conclusively exclude the contribution of cell proliferation, and this will be pursued in future investigations.

In addition, we also analyzed the Golgi proteome and N-glycosylated proteome. The results showed that several proteins involved in cell wall metabolism were differentially expressed. Notably, at the level of protein post-translational modifications, proteins can undergo glycosylation under the action of glycosyltransferases. The glycosylated proteomic results revealed that ClURGT4 mutation resulted in changes in the levels and glycosylation patterns of several proteins involved in cell wall degradation (pectin lyase) and lignification (peroxidase). Pectin, as a complex polysaccharide widely present in plant cell walls, is primarily composed of GalA polymers. Pectin lyase primarily cleaves pectin polymers through a trans-elimination reaction, and it can degrade pectin, affecting the integrity of cell walls and adhesion between cells to control cell expansion. Therefore, downregulation of pectin lyase may indirectly affect RG-II by reducing the content of GalA, and inhibit cell expansion, thereby decreasing watermelon biomass and fruit size. Peroxidase primarily participates in the synthesis of lignin in the cell wall, the modification of cell wall structure, and the response to external environmental stimuli. By catalyzing the synthesis of substances such as

lignin, peroxidase affects the structure and composition of the cell wall, which may indirectly influence cell growth and size. Surprisingly, complete loss of complex N-glycan in *Arabidopsis* has been reported to have little impact on plant growth and development [40,41]. In contrast, many O-glycosylated proteins, such as arabinogalactan proteins (AGPs), are known to be very important for growth and development [42,43], and glycosylation of AGPs is essential [44]. AGPs are rich in both Gal and Rha, and it would be interesting to determine if AGP glycosylation is altered in the *clurgt4* mutants and in the corresponding *aturgt4*, *-5*, and *-6* mutants in *Arabidopsis*. Unfortunately, the analysis of O-glycosylation patterns is not straightforward. Thus, it is still unclear how the glycosylation patterns of pectin lyase and peroxidase proteins regulate cell size, and more detailed research is needed in the future to clarify the role of their glycosylation patterns. On this basis, transgenic approaches are needed to further elucidate how ClURGT4-mediated alterations in specific cell wall metabolic genes and their glycosylation patterns regulate watermelon fruit size and biomass. Additionally, exploring the interaction proteins and upstream regulatory mechanisms of the membrane protein ClURGT4 through more methods and technological systems to promote the development and application of sugar transporters remains a key and challenging research focus in the future.

5. Conclusion

In watermelon, the Golgi-localized ClURGT4 transports UDP-Rha and UDP-Gal, and *clurgt4* mutants show smaller fruit size and decreased biomass, accompanied by reduced Gal, Rha, and GalA contents in the cell wall. Further glycoproteomics analysis revealed that cell wall degradation and lignification pathways were modified at the post-translational level, which may indirectly lead to reduced cell size. These findings provide new insights into the function of NSTs in fruit crops, and show that ClURGT4 is a valuable genetic target with potential for improving crop yield through molecular design breeding.

CRediT authorship contribution statement

Ge Gao: Project administration, Resources, Software, Supervision, Visualization, Writing – original draft. **Shengjin Liao:** Data curation, Methodology, Software. **Shouwei Tian:** Project administration, Resources, Software. **Xiujing Feng:** Methodology, Resources. **Chen Zhang:** Validation, Visualization. **Jie Zhang:** Supervision. **Maoying Li:** Conceptualization, Data curation. **Shaogui Guo:** Supervision. **Yongtao Yu:** Methodology, Project administration. **Jinfang Wang:** Investigation. **Guoyi Gong:** Validation. **Haiying Zhang:** Visualization. **Henrik V. Scheller:** Methodology, Validation, Visualization, Writing – review & editing. **Yong Xu:** Conceptualization, Funding acquisition, Investigation, Methodology, Project administration. **Yi Ren:** Conceptualization, Data curation, Funding acquisition, Methodology, Project administration, Resources, Supervision, Validation, Visualization, Writing – review & editing.

Declaration of competing interest

The authors declare that they have no known competing financial interests or personal relationships that could have appeared to influence the work reported in this paper. Yong Xu is an Editorial Board Member of *Agriculture Communications*, but he had no involvement in the peer review of this article and had no access to information regarding its whole review process.

Acknowledgments

This research was supported by grants from the National Natural Science Foundation of China (32341046), Beijing Rural Revitalization Agricultural Science and Technology Project (NY2401130126), the Scientist Training Program of BAAFS (JKZX202211), Beijing Academy of Agriculture and Forestry Sciences Exploratory Project (TSXM202509), Project for Scientific and Technological Innovation Capability Building of the Beijing Academy of Agriculture and Forestry Sciences (2026-2027), construction of cucurbits collaboration and innovation center (XTCX202301), Innovation and Development Program of Beijing Vegetable Research Center (KYCX202501). Work at the DOE Joint BioEnergy Institute (http://www.jbei.org) was supported by the U.S. Department of Energy, Office of Science, Biological and Environmental Research Program, through contract DE-AC02-05CH11231 between Lawrence Berkeley National Laboratory and the U. S. Department of Energy.

Appendix A. Supplementary data

Supplementary data to this article can be found online at https://doi.org/10.1016/j.agrcom.2026.100149.

Data availability

The data that support the findings of this study are available in the Supporting Information of this article.

References

[1] Tang Y, Lu L, Huang X, Zhao D, Tao J. The herbaceous peony transcription factor WRKY41a promotes secondary cell wall thickening to enhance stem strength. Plant Physiol 2022;191(1):428–45.
[2] Zhang W, Qin W, Li H, Wu A. Biosynthesis and transport of nucleotide sugars for plant hemicellulose. Front Plant Sci 2021;12:723128.
[3] Bakker H, Routier F, Oelmann S, Jordi W, Lommen A, Gerardy-Schahn R, et al. Molecular cloning of two *Arabidopsis* UDP-galactose transporters by complementation of a deficient Chinese hamster ovary cell line. Glycobiology 2005;15(2):193–201.
[4] Zhang B, Liu X, Qian Q, Liu L, Dong G, Xiong G, et al. Golgi nucleotide sugar transporter modulates cell wall biosynthesis and plant growth in rice. Proc Natl Acad Sci USA 2011;108(12):5110–5.
[5] Handford M, Rodríguez-Furlán C, Marchant L, Segura M, Gómez D, Alvarez-Buylla E, et al. *Arabidopsis thaliana* AtUTr7 encodes a golgi-localized UDP-glucose/UDP-galactose transporter that affects lateral root emergence. Mol Plant 2012;5(6):1263–80.
[6] O'Neill MA, Eberhard S, Albersheim P, Darvill AG. Requirement of borate cross-linking of cell wall rhamnogalacturonan II for *arabidopsis* growth. Science 2001;294(5543):846–9.
[7] Janse van Rensburg HC, Van den Ende W. UDP-Glucose: a potential signaling molecule in plants? Front Plant Sci 2018;8:2230.
[8] Wai C, Zhang J, Jones T, Nagai C, Ming R. Cell wall metabolism and hexose allocation contribute to biomass accumulation in high yielding extreme segregants of a Saccharum interspecific F2 population. BMC Genom 2017;18(1):773.
[9] Norambuena L, Nilo R, Handford M, Reyes F, Marchant L, Meisel L, et al. AtUTr2 is an *Arabidopsis thaliana* nucleotide sugar transporter located in the Golgi apparatus capable of transporting UDP-galactose. Planta 2005;222(3):521–9.
[10] Knappe S, Flügge UI, Fischer K. Analysis of the plastidic *phosphate translocator* gene family in Arabidopsis and identification of new *phosphate translocator*-Homologous transporters, classified by their putative substrate-binding site. Plant Physiol 2003;131(3):1178–90.
[11] Rautengarten C, Ebert B, Moreno I, Temple H, Herter T, Link B, et al. The Golgi localized bifunctional UDP-rhamnose/UDP-galactose transporter family of *Arabidopsis*. Proc Natl Acad Sci USA 2014;111(31):11563–8.
[12] Ebert B, Rautengarten C, Guo X, Xiong G, Stonebloom S, Smith-Moritz AM, et al. Identification and characterization of a Golgi-localized UDP-xylose transporter family from *Arabidopsis*. Plant Cell 2015;27(4):1218–27.
[13] Chen D, Kamran M, Chen S, Xing J, Qu Z, Liu C, et al. Two nucleotide sugar transporters are important for cell wall integrity and full virulence of Magnaporthe oryzae. Mol Plant Pathol 2023;24(4):374–90.
[14] Tian X, Li X, Zhou W, Ren Y, Wang Z, Liu Z, et al. Transcription factor OsWRKY53 positively regulates brassinosteroid signaling and plant architecture. Plant Physiol 2017;175(3):1337–49.
[15] Kong Q, Yuan J, Gao L, Zhao S, Jiang W, Huang Y, et al. Identification of suitable reference genes for gene expression normalization in qRT-PCR analysis in watermelon. PLoS One 2014;9(2):e90612.
[16] Omasits U, Ahrens CH, Müller S, Wollscheid B. Protter: interactive protein feature visualization and integration with experimental proteomic data. Bioinformatics 2014;30(6):884–6.
[17] Arrivault S, Guenther M, Ivakov A, Feil R, Vosloh D, van Dongen JT, et al. Use of reverse-phase liquid chromatography, linked to tandem mass spectrometry, to profile the Calvin cycle and other metabolic intermediates in *Arabidopsis* rosettes at different carbon dioxide concentrations. Plant J 2009;59(5):826–39.
[18] Ito J, Herter T, Baidoo EEK, Lao J, Vega-Sánchez ME, Smith-Moritz AM, et al. Analysis of plant nucleotide sugars by hydrophilic interaction liquid chromatography and tandem mass spectrometry. Anal Biochem 2014;448:14–22.

[19] Suo J, Li H, Ban Q, Han Y. Characteristics of chilling injury-induced lignification in kiwifruit with different sensitivities to low temperatures. Postharvest Biol Technol 2018;135:8–18.
[20] Yang Y, Liu X, Shen C, Lin Y, Yang P, Qiao L. In silico spectral libraries by deep learning facilitate data-independent acquisition proteomics. Nat Commun 2020;11(1):1–11.
[21] Ntai L, Toby TK, LeDuc RD, Kelleher NL. A method for label-free, differential top-down proteomics. Methods Mol Biol 2016;1410:121–33.
[22] Bradford MM. A rapid and sensitive method for the quantitation of microgram quantities of protein utilizing the principle of protein-dye binding. Anal Biochem 1976;72:248–54.
[23] Saez-Aguayo S, Parra-Rojas JP, Sepúlveda-Orellana P, Celiz-Balboa J, Arenas-Morales V, Sallé C, et al. Transport of UDP-rhamnose by URGT2, URGT4, and URGT6 modulates rhamnogalacturonan-I length. Plant Physiol 2021;185(3):914–33.
[24] Xiao G, Zhou J, Lu X, Huang R, Zhang H. Excessive UDPG resulting from the mutation of *UAP1* causes programmed cell death by triggering reactive oxygen species accumulation and caspase-like activity in rice. New Phytol 2018;217(1):332–43.
[25] Yi J, Wang Y, Ma X, Zhang J, Zhao M, Huang X, et al. *LcERF2* modulates cell wall metabolism by directly targeting a UDP-glucose-4-epimerase gene to regulate pedicel development and fruit abscission of litchi. Plant J 2021;106(3):801–16.
[26] Guo T, Chen K, Dong N, Shi C, Ye W, Gao J, et al. *GRAIN SIZE AND NUMBER1* negatively regulates the OsMKKK10-OsMKK4-OsMPK6 cscade to coordinate the trade-off between grain number per panicle and grain size in rice. Plant Cell 2018;30(4):871–88.
[27] Xu R, Duan P, Yu H, Zhou Z, Zhang B, Wang R, et al. Control of grain size and weight by the OsMKKK10-OsMKK4-OsMAPK6 signaling pathway in rice. Mol Plant 2018;11(6):860–73.
[28] Vanholme R, Demedts B, Morreel K, Ralph J, Boerjan W. Lignin biosynthesis and structure. Plant Physiol 2010;153(3):895–905.
[29] Zhang B, Gao Y, Zhang L, Zhou Y. The plant cell wall: biosynthesis, construction, and functions. J Integr Plant Biol 2021;63(1):251–72.
[30] Yang C, Wang C, Singh S, Fan N, Liu S, Zhao L, et al. Golgi-localised manganese transporter PML3 regulates *arabidopsis* growth through modulating Golgi glycosylation and cell wall biosynthesis. New Phytol 2021;231(6):2200–14.
[31] Handford M, Rodriguez-Furlán C, Orellana A. Nucleotide-sugar transporters: structure, function and roles *in vivo*. Braz J Med Biol Res 2006;39(9):1149–58.
[32] Orellana A, Moraga C, Araya M, Moreno A. Overview of nucleotide sugar transporter gene family functions across multiple species. J Mol Biol 2016;428(16):3150–65.
[33] Wang J, Ji Q, Jiang L, Shen S, Fan Y, Zhang C. Overexpression of a cytosol-localized rhamnose biosynthesis protein encoded by *Arabidopsis* RHM1 gene increases rhamnose content in cell wall. Plant Physiol Biochem 2009;47(2):86–93.
[34] Fabrissin I, Cueff G, Berger A, Granier F, Sallé C, Poulain D, et al. Natural variation reveals a key role for rhamnogalacturonan I in seed outer mucilage and underlying genes. Plant Physiol 2019;181(4):1498–518.
[35] Reiter WD, Chapple C, Somerville CR. Mutants of *Arabidopsis thaliana* with altered cell wall polysaccharide composition. Plant J 1997;12(2):335–45.
[36] Bouton S, Leboeuf E, Mouille G, Leydecker MT, Talbotec J, Granier F, et al. *QUASIMODO1* encodes a putative membrane-bound glycosyltransferase required for normal pectin synthesis and cell adhesion in *Arabidop*sis. Plant Cell 2002;14(10):2577–90.
[37] Nguema-Ona E, Andeme-Onzighi C, Aboughe-Angone S, Bardor M, Ishii T, Lerouge P, et al. The *reb1-1* mutation of Arabidopsis. Effect on the structure and localization of galactose-containing cell wall polysaccharides. Plant Physiol 2006;140(4):1406–17.
[38] Kaczmarska A, Pieczywek PM, Cybulska J, Zdunek A. Structure and functionality of Rhamnogalacturonan I in the cell wall and in solution: a review. Carbohydr Polym 2022;278:118909.
[39] Funakawa H, Miwa K. Synthesis of borate cross-linked rhamnogalacturonan II. Front Plant Sci 2015;6:223.
[40] Strasser R, Stadlmann J, Svoboda B, Altmann F, Glössl J, Mach L. Molecular basis of N-acetylglucosaminyltransferase I deficiency in *Arabidopsis thaliana* plants lacking complex N-glycans. Biochem J 2005;387(2):385–91.
[41] Ebert B, Rautengarten C, McFarlane HE, Rupasinghe T, Zeng W, Ford K, et al. A Golgi UDP-GlcNAc transporter delivers substrates for *N*-linked glycans and sphingolipids. Nat Plants 2018;4(10):792–801.
[42] Kaur D, Held MA, Smith MR, Showalter AM. Functional characterization of hydroxyproline-O-galactosyltransferases for *Arabidopsis* arabinogalactan-protein synthesis. BMC Plant Biol 2021;21(1):590.
[43] Ma Y, Johnson K. Arabinogalactan proteins-multifunctional glycoproteins of the plant cell wall. Cell Surf 2023;9:100102.
[44] Geshi N, Johansen JN, Dilokpimol A, Rolland A, Belcram K, Verger S, et al. A galactosyltransferase acting on arabinogalactan protein glycans is essential for embryo development in *Arabidopsis*. Plant J 2013;76(1):128–37.